Taylor Galerkin Pressure Correction (TGPC) Finite Element Method for Incompressible Newtonian Cable-Coating Flows

Alaa H. Al-Muslimawi
Department of Mathematics,
College of Science, University of Basrah
Basrah, Iraq
alaamath73@gmail.com

Received May. 23, 2018. Accepted for publication Jun. 28, 2018
DOI: http://dx.doi.org/ 10.31642/JoKMC/2018/050203

Abstract- *Based on Taylor Galerkin /pressure-correction (TGPC) finite element method, this work is concerned with numerical study for incompressible Newtonian cable coating flows. The fluid motion is described by using the Naiver-Stoke equations, which include two essential differential equations. One of them is the equation for conservation of mass and the other one is the equation of conservation of momentum equations.*

Moreover, this study shows the free surface location methodology to determine the free surface position, and the boundary conditions. The Phan-Thien (dh/dt) scheme is applied to calculate the change in the free-surface position. A number of computational investigations have been achieved to see the effect of different factors on the processing of coating. This includes investigating the influence of variation in surface tension on the shear rate and strain-rate stabilisation approach.

Keywords- ***finite element method; Galerkin method; surface tension; cable coating***

I. INTRODUCTION

A semi-implicit time-stepping Taylor-Galerkin Pressure-Correction finite element (TGPC) algorithm is employed to analyze the Newtonian coating fluid. The conservation of mass and time dependent of momentum equations are the essential components of this model, as they describe the behavior of the fluid. The model of differential equations under consideration is presented in cylindrical coordinates system (Axisymmetric flow). In this context, considering flow in annular two dimensional, axisymmetric cylindrical coordinate frames (laminar flow over circular conduit) is investigated (see [1]).

In the industrial field, cable coating process represents an important commercial issue. This process demands falling a molten polymer over a moving cable, and then cooling trough for the extruded cable [2-4]. Recently, two types of coating designs have been utilized in the commercial field; tube-tooling and pressure-tooling [4-5]. In this study, the-tooling extrusion coating problem is treated numerically. Moreover, this investigation introduces the free surface flow

matter, which is a major challenge in numerical studies. In this context, a particle-tracking/surface height-function technique (*dh/dt)*, developed by Phan-Thien [6] is implemented to treat the free-surface movement. This method is applied based on two steps to get a suitable shape for the extrudate swell. Starting the solution as a fixed position problem (no free surface movement), and then using that solution as initial condition to solve the problem when the movement of surfaces is allowed.

Numerically, several studies are conducted to solve this type of problems (see foe example Caswell and Tanner [7], Sun et al. [8], Kuyl [9, 10] and Al-Muslimawi [11]). In addition, this subject under boundary conditions is studied by many authors. Under this concept, Ngamaramvaranggul and Webster [12] and Al-Muslimawi [13] used a TGPC finite element method to analyze the wire and cable coating problems for incompressible Newtonian flows, where the free surface issue is appeared strongly within TGPC method.

Analytically, Slattery *et al.* [14] has a theoretical procedure wire-coating problem. Also, the analytic solution for same problem is discussed by Hade and Giacomin [16].

In a recent article, the numerical solution for incompressible Newtonian cable coating flows with free surface movement is discussed based on (TGPC) method. Two computational tests have been performed to assess the effect of various features on the coating procedure within the draw-down section (DDS) of the flow. This includes investigating the effect of variation in surface tension and strain-rate stabilisation approach

II. MATHEMATICAL MODELLING

For incompressible Newtonian isothermal flow, the continuity equation and the momentum equation in the cylindrical components can be given respectively as:

$$\nabla \cdot u = 0. \tag{1}$$

Where, u represents the velocity of fluid.

The balance of momentum reduces to

$$\rho \frac{\partial u}{\partial t} = \nabla \cdot \sigma - \rho u.\nabla u\,,$$

$$\sigma = -pI + 2\mu_s d\ . \tag{2}$$

Where, ρ is the fluid density, σ the total-stress tensor and $d = (L + L^T)/2$, with $L^T = \nabla \mathrm{u}$ is the Euler rate-of-deformation tensor .

In the cylindrical components these equations can be re-written as

$$\frac{1}{r}\frac{\partial r u_r}{\partial r} + \frac{1}{r}\frac{\partial u_\theta}{\partial \theta} + \frac{\partial u_z}{\partial z} = 0. \tag{3}$$

***r* -component**

$$\frac{\partial u_r}{\partial t} + u_r \frac{\partial u_r}{\partial r} + \frac{u_\theta}{r}\frac{\partial u_r}{\partial \theta} - \frac{u_\theta^2}{r} + u_z \frac{\partial u_r}{\partial z} =$$
$$-\frac{1}{\rho}\frac{\partial p}{\partial r} + \frac{\mu_s}{\rho}\left(\frac{1}{r}\frac{\partial}{\partial r}\left(r\frac{\partial u_r}{\partial r}\right) - \frac{u_r}{r^2} + \right. \tag{4}$$
$$\left.\frac{1}{r^2}\frac{\partial^2 u_r}{\partial \theta^2} - \frac{2}{r^2}\frac{\partial u_\theta}{\partial \theta} + \frac{\partial^2 u_r}{\partial z^2}\right),$$

***θ* -component**

$$\frac{\partial u_\theta}{\partial t} + u_r \frac{\partial u_\theta}{\partial r} + \frac{u_\theta}{r}\frac{\partial u_\theta}{\partial \theta} + \frac{u_r u_\theta}{r} + u_z \frac{\partial u_\theta}{\partial z} =$$
$$-\frac{1}{r\rho}\frac{\partial p}{\partial \theta} + \frac{\mu_s}{\rho}\left(\frac{1}{r}\frac{\partial}{\partial r}\left(r\frac{\partial u_\theta}{\partial r}\right) - \frac{u_\theta}{r^2}\right.$$
$$\left. + \frac{1}{r^2}\frac{\partial^2 u_\theta}{\partial \theta^2} + \frac{2}{r^2}\frac{\partial u_r}{\partial \theta} + \frac{\partial^2 u_\theta}{\partial z^2}\right), \tag{5}$$

***z* -component**

$$\frac{\partial u_z}{\partial t} + u_r \frac{\partial u_z}{\partial r} + \frac{u_\theta}{r}\frac{\partial u_z}{\partial \theta} + u_z \frac{\partial u_z}{\partial z} = -\frac{1}{\rho}\frac{\partial p}{\partial z} +$$
$$\frac{\mu_s}{\rho}\left(\frac{1}{r}\frac{\partial}{\partial r}\left(r\frac{\partial u_z}{\partial r}\right) + \frac{1}{r^2}\frac{\partial^2 u_z}{\partial \theta^2} + \frac{\partial^2 u_z}{\partial z^2}\right).$$

(6)

where, u_r, u_θ and u_z represent the velocity in r direction, θ direction and z direction. Also, p and ρ represent the pressure and density of the fluid and μ_s is the solvent viscosity. Further, the equation can also be defined by the non-dimensional groups of Reynolds number (Re), and viscosity (β), which are characterized by the scales of velocity (U), length (L) and density (ρ) as, $Re = \rho \frac{Ul}{\mu_s}$ and $\beta = \mu_s$ (for more details see [14], [15]).

III. NUMERICAL METHOD

A. TIME DISCRETISATION

A Taylor Galerkin Pressure Correction time step method (TGPC) is implemented in this investigation to treat the equations (1-2). This numerical technique is introduced by Townsend and Webster (see [17]) based on Lax_Wendroff time stepping.

Rewriting the momentum equation (2) in the non-dimensional groups of Reynolds number (Re), and viscosity (β) as

$$\frac{\partial u}{\partial t} = \frac{1}{\mathrm{Re}}\left[\nabla\cdot(2\beta d) - \mathrm{Re}\, u.\nabla u - \nabla p\right]. \quad (7)$$

Using Taylor expansion of u around t^n then,

$$u^{n+1} = u^n + \Delta t\left[\frac{1}{\mathrm{Re}}\left[\nabla\cdot(2\beta d) - \mathrm{Re}\, u.\nabla u - \nabla p\right]\right]^n + \frac{(\Delta t)^2}{2}\left[\frac{\partial}{\partial u}\left(\frac{1}{\mathrm{Re}}\left[\nabla\cdot(2\beta d) - \mathrm{Re}\, u.\nabla u - \nabla p\right]\right)\right]^n \left[\frac{1}{\mathrm{Re}}\left[\nabla\cdot(2\beta d) - \mathrm{Re}\, u.\nabla u - \nabla p\right]\right]^n \quad (8)$$

Now, by the tow steps of Lax_Wendroff approach we gather the velocity as,

Step 1:

$$u^{n+\frac{1}{2}} = u^n + \frac{\Delta t}{2\,\mathrm{Re}}\left[\left(\nabla\cdot(2\beta d) - \mathrm{Re}\, u.\nabla u\right)^n - \nabla p^n\right] \quad (9a)$$

Step 2:

$$u^{n+1} = u^n + \frac{\Delta t}{\mathrm{Re}}\left[\left(\nabla\cdot(2\beta d) - \mathrm{Re}\, u.\nabla u\right)^{n+\frac{1}{2}} - \nabla p^{n+\frac{1}{2}}\right] \quad (9b)$$

In contrast, the pressure $p^{n+\frac{1}{2}}$ in Eq. (9b) is defined by

$$p^{n+\frac{1}{2}} = \theta p^{n+1} + (1-\theta)p^n, \quad (10)$$

Such that, the Eq(9b) can be written as

$$u^{n+1} = u^n + \frac{\Delta t}{\mathrm{Re}}[\left(\nabla\cdot(2\beta d) - \mathrm{Re}\, u.\nabla u\right)^{n+\frac{1}{2}} - \theta\nabla p^{n+1} - (1-\theta)\nabla p^n]. \quad (11)$$

Suppose u^* is an intermediate velocity such that

$$u^* = u^n + \frac{\Delta t}{\mathrm{Re}}\left[\left(\nabla\cdot(2\beta d) - \mathrm{Re}\, u.\nabla u\right)^{n+\frac{1}{2}} - \nabla p^n\right]. \quad (12)$$

From Eq.(11) and Eq.(12), we have

$$\nabla^2(p^{n+1} - p^n) = \frac{\mathrm{Re}}{\theta\Delta t}\nabla\cdot u^*, \quad (13a)$$

$$u^{n+1} = u^* - \frac{\theta\Delta t}{\mathrm{Re}}\nabla(p^{n+1} - p^n), \quad (13b)$$

Thus, from (9a), (9b), (13a) and (13b) we have the following stages

Stage 1a:

$$\frac{2\,\mathrm{Re}}{\Delta t}(u^{n+\frac{1}{2}} - u^n) = \left[\left(\nabla\cdot(2\beta d) - \mathrm{Re}\, u.\nabla u\right)^n - \nabla p^n\right], \quad (14a)$$

Stage 1b:

$$\frac{\mathrm{Re}}{\Delta t}(u^* - u^n) = \left[\left(\nabla\cdot(2\beta d) - \mathrm{Re}\, u.\nabla u\right)^{n+\frac{1}{2}} - \nabla p^n\right], \quad (14b)$$

Stage 2: $\nabla^2(p^{n+1} - p^n) = \frac{\mathrm{Re}}{\theta\Delta t}\nabla\cdot u^*$, (14c)

Stage 3: $u^{n+1} = u^* - \frac{\theta \Delta t}{\mathrm{Re}} \nabla (p^{n+1} - p^n)$. (14d)

B. FINITE ELEMENT SCHEME

To apply the (TGPC) method the approximations for velocity and pressure fields based on respective shape functions ψ_i and ϕ_j ($i = 1,2,\ldots,\epsilon$, total number of nodes including mid-side points and $j = 1,2,3$, number of vertex nodes only) are introduced as

$$u(x,t) = u_j(t)\phi_j(x), \quad j = 1,\ldots,6,$$
$$p(x,t) = p_k(t)\psi_k(x), \quad k = 1,\ldots,3. \qquad (15)$$

Such that, the shape functions, $\phi_j(x)$ are selected as piecewise quadratic basis functions and $\psi_k(x)$ as piecewise linear basis functions. Then the stages (14a)-(14c) can be written in the matrix-form as

Step 1a: $[\frac{2\,\mathrm{Re}}{\Delta t} M + \frac{1}{2} S](U^{n+\frac{1}{2}} - U^n) = \{-[S + \mathrm{Re}\, N(U)]U + L^T P\}^n$, (16a)

Step 1b:

$$[\frac{\mathrm{Re}}{\Delta t} M + \frac{1}{2} S](U^* - U^n) = \{-SU + L^T p\}^n - \mathrm{Re}[N(U)U]^{n+\frac{1}{2}}, \qquad (16b)$$

Step 2: $K(P^{n+1} - P^n) = -\frac{\mathrm{Re}}{\theta \Delta t} LU^*$, (16c)

Step 3: $\frac{\mathrm{Re}}{\Delta t} M(U^{n+1} - U^*) = \theta L^T (P^{n+1} - P^n)$. (16d)

Where, M is the mass matrix, S is the momentum diffusion matrix, K is the pressure stiffness matrix, $N(U)$ is the convection matrix and L is the divergence/ pressure gradient matrix. In a matrix notation

$$M_{ij} = \int_\Omega \phi_i . \phi_j \, d\Omega \quad , \quad K_{ij} = \int_\Omega \nabla \psi_i \nabla \psi_j \, d\Omega \quad ,$$
$$N(U)_{ij} = \int_\Omega \phi_i (U_k^l \frac{\partial \phi_j}{\partial x_k}) \, d\Omega, (L)_{ij} = \int_\Omega \psi_i \frac{\partial \phi_j}{\partial x_k} \, d\Omega \quad ,$$
$$(S)_{ij} = \int_\Omega \frac{\partial \phi_i}{\partial x_k} \frac{\partial \phi_j}{\partial x_k} + (\frac{\partial \phi_j}{\partial x_k})^T \, d\Omega$$

C. STRAIN-RATE STABILISATION SCHEME

To see the effect of some factors on the present numerical solution of cable coating problem, the Strain-Rate Stabilisation technique (d-d_c) is applied for the momentum and continuity equations. This scheme is achieved by adding the following term to the momentum equation

$$2\alpha(d - d_c), \qquad (17)$$

where, D_c is the approximate finite element rate of deformation tensor solution, and α is an stabilization factor. In this study α=0.25, α=0.5 is used.

The numerical algorithm will be changed under the consideration of this scheme. The main change is appeared in stages (16a) and (16b), which modified to:

Step 1a: $[\frac{2\,\mathrm{Re}}{\Delta t} M + \frac{1}{2} S](U^{n+\frac{1}{2}} - U^n) = \{-[S + \mathrm{Re}\, N(U)]U + L^T P\}^n$ +SRS-term, (18a)

Step 1b:

$$[\frac{\mathrm{Re}}{\Delta t} M + \frac{1}{2} S](U^* - U^n) = \{-SU + L^T p\}^n - \mathrm{Re}[N(U)U]^{n+\frac{1}{2}} \text{ +SRS-term}, \qquad (18b)$$

D. SURFACE TENSION EFFECT

The second factor in this study is the surface tension, thus problem can be solved under this factor by applying following boundary condition

$$\sigma.n = -p_a.n - Ca^{-1}\left(\frac{1}{R_1}+\frac{1}{R_2}\right).n \quad (19)$$

where, p_a is the ambient surrounding pressure level, R_1 and R_2 are the radius of the free surface curvature and $\boldsymbol{n}$ is the normal vector.

E. FREE-SURFACE PROCEDURE

To treat the free surface nodal movement, the Phan-Thien (dh/dt) method is chosen for the current study. In this method the calculation of the new position of the nodal is restricted in the radial motion only to be suitable with the nature of the problem under consideration. This procedure is satisfied via solution of the following first-order differential equation [18-19]:

$$\frac{\partial h}{\partial t} + v_z \frac{\partial h}{\partial z} - u_r = 0. \quad (20)$$

Where, u_r, v_z are the radial and axial velocities respectively, and h represents the height.

IV. PROBLEM SPECIFICATION

The design geometry of our problem (tube-tooling) is shown in Figure 1. A schematic representation for the draw-down section (DDS) and cable region of tube-tooling design with the finite element mesh is presented in this Figure. Also, the relative dimensions of the mesh are provided in Table 1. All the found results are for Newtonian case with Re=10^{-4}.

***Boundary conditions (BCs)*:** The setting of *BCs* of the present problem is laid as follows:

(a) No-slip BC_s is applied on the die walls.

(b) For DD section and cable area we had:

(i) slip BC_s is applied on the top and bottom surface without a pressure.

(ii) Plug flow is forced in the cable region.

Table 1: Mesh characteristic parameters

Elements	Nodes	Degrees of freedom (u, p)
2004	4355	27306

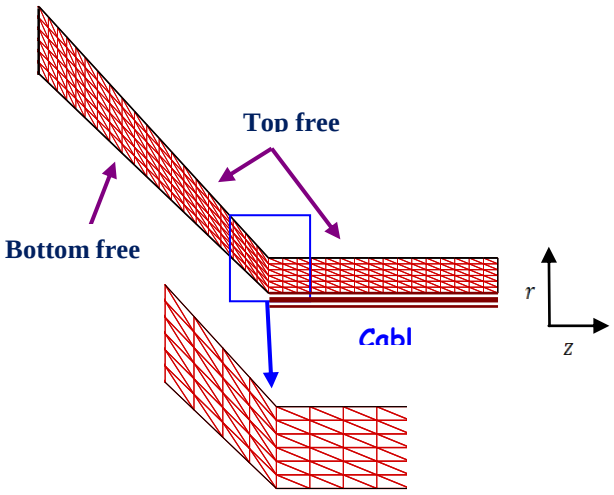

Figure 1: Schematic diagram for draw down

V. NUMERICAL RESULTS

The (TGBC) numerical results for DDS of cable coating problem are presented. The study concerned with the shape of draw down section, which represents the major challenge in this work. In addition, the influence of two important factors in this process; surface tension and strain-rate stabilisation approach also are provided in this study.

The shape for the DDS, with re-meshing in the essential locations at the exit of die and draw-down section, is shown in Figure 2. Plug flow applies at the domain outlet and there is distinct contact point movement observed (reducing the length of the DDS). The contact

point is traversed smoothly, thus any node on the bottom free surface touches with the cable.

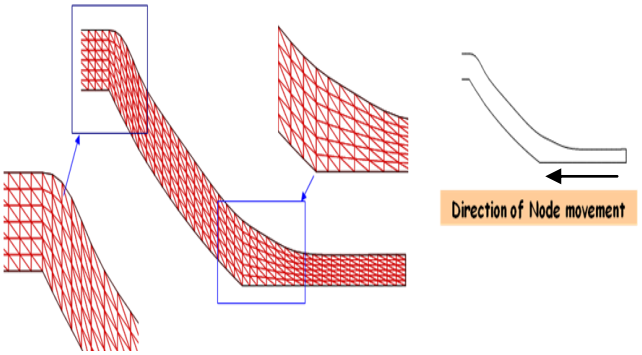

Figure 2: Top and bottom free surface movement

Pressure field and profile along the draw-down centre are shown in Figure 3, with a zoomed die exit section. The maximum and minimum levels in pressure are illustrated in this Figure around the die exit. From the pressure profile, one can notice some changes are occurred in the draw-down and the coating, with a rising trend upon entry to the coating.

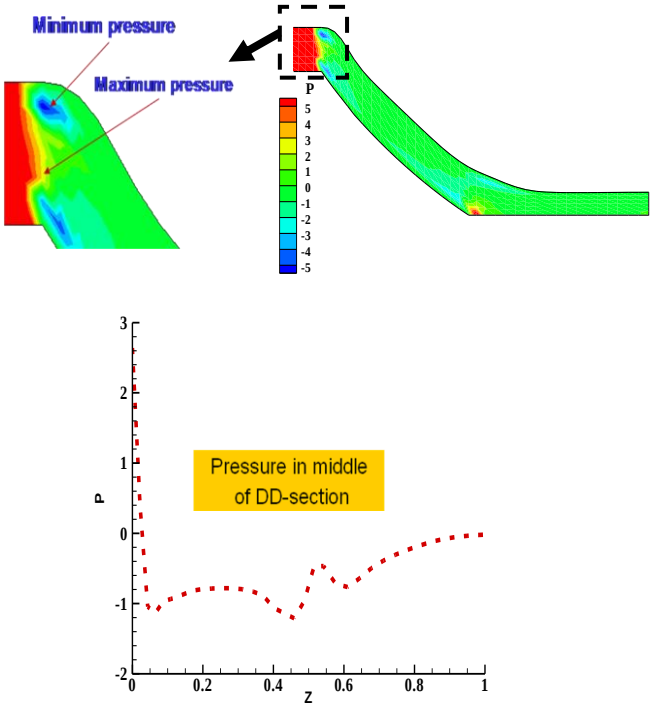

Figure 3: Pressure field and profile for draw down section

Axial and radial velocity fields with sampled profiles (top surface, bottom surface, core flow) are recorded in Figure 4. At the various positions throughout the DDS, different levels of velocities are displayed. In the axial velocity profile, the smallest value is noted around the entry to the draw-down, which then rises and relaxes throughout the cable coating region. While, for the radial velocity, there is a decline from the die-exit, to finally reaching a minimum value observed near the contact point on the bottom surface of this section. Radial velocity for the bottom surface at the exit of the DDS is about twice the magnitude (negative in sign) of that for the top and central sections; while, there is sharp adjustment in radial velocity on wetting the cable. Hence, plug flow conditions are clearly seen to apply in the coating.

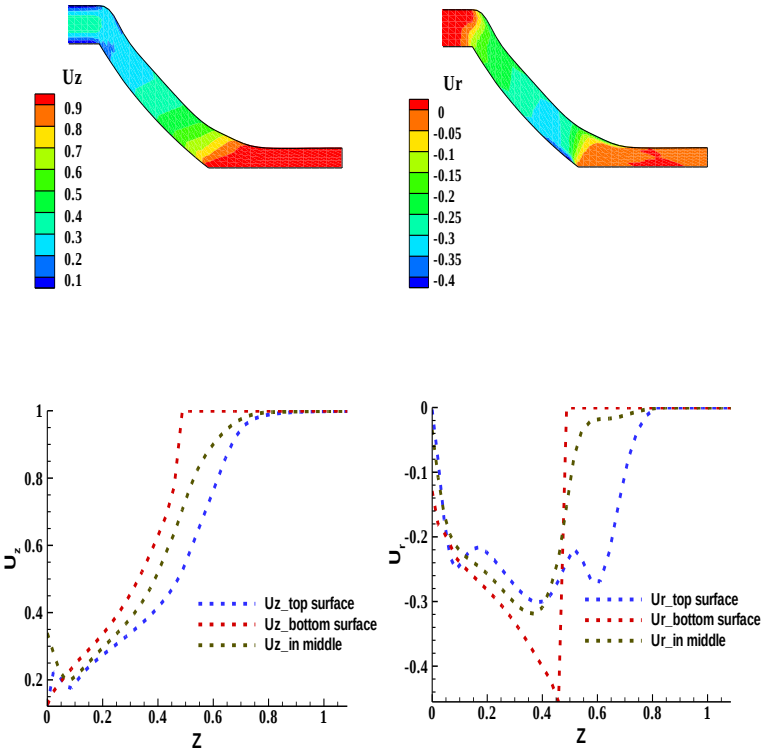

Figure 4: Pressure fields and profiles for draw down section

(d-dc) scheme: This problem is solved by applying (*d-dc*) stabilization scheme, including factors α=0.25, α=0.5. The study is focused on the influence of this technique on the shape of DDS and the level of swell-exist compared to that without (*d-dc*).

The corresponding swelling data and zoomed view of the die are provided in Figure 5. From these results, a slighter level of swelling is observed when the singularity is additionally accounted for through the (d-d_c) realisation. This is particularly well noticeable in the comparison against the previous results without (d-d_c) treatment. Furthermore, one can see the outcome of (d-d_c) on the contact point solution, which follows slower movement under (d-d_c).

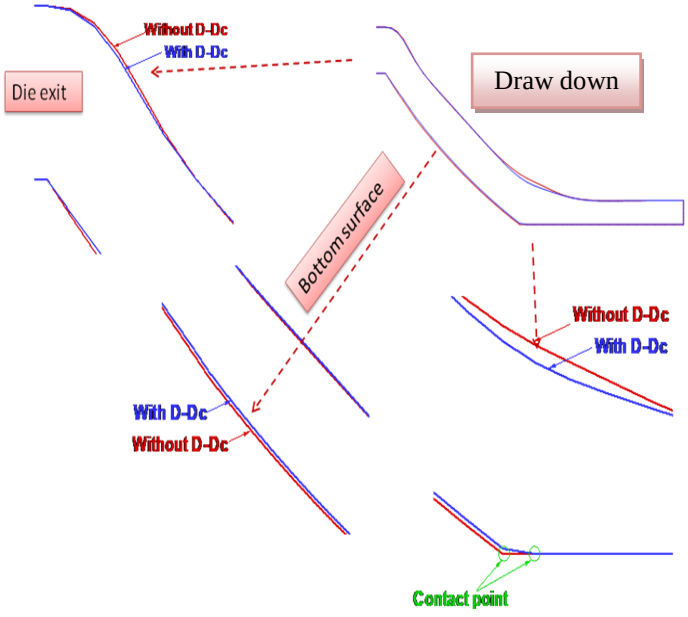

Figure 5: d-dc effect on geometry shape of draw down section

Surface tension effect (st): In contrast to the foregoing of the study, the problem is solved with inclusion of surface tension. Comparative data are presented on pressure in Figure 6a, along the draw-down centre with/without surface tension effects. Findings indicate that there is insignificant change apparent with surface tension inclusion; yet there is some slight change noticed near the contact point region.

Shear-rate (Gamma) profiles at the top and bottom free surface are illustrated in Figure 6b, with/without surface tension effects. The results reflect that overall, insignificant change is detected under surface tension influence, bar at the bottom surface near the contact point. There, Gamma reaches a peak value of around 35 units, which is an increase of 30% from that for instance without surface tension (25 units). The same response is gathered in shear stress (Trz), with reduction of contact-point peak value on the bottom surface due to surface tension, from around 70 to 40 units (see Figure 6c).

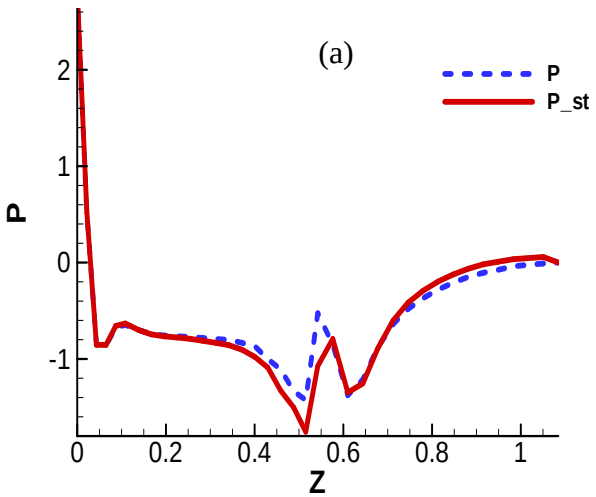

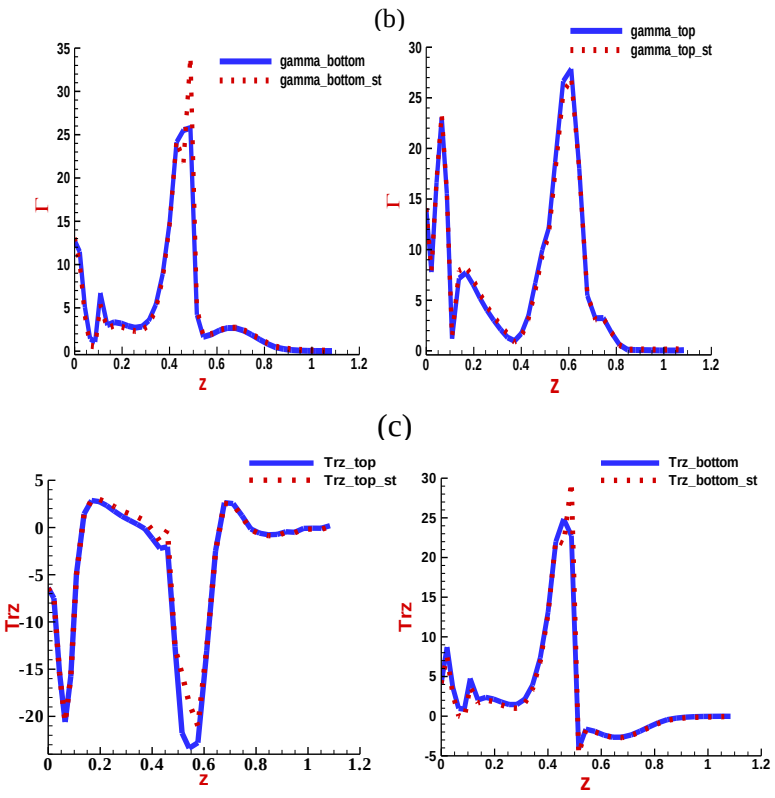

Figure 6: Surface tension effects

VI. CONCLUSION

This study is covered the analysis of the draw-down section, with different scenarios. The shape of top and bottom surfaces and the behaviour of the velocity and pressure have been investigated throughout the draw-down section. Study of some factors also presented, which include the influence of the surface tension and that of the strain-rate stabilisation approach.

The influence of singularity capturing on the die-exit solution has been explored successfully using the (*d-dc*) technique. In this manner, A significant impact on the levels of die-swell that can occurred in such treatment is also shown. Finally, this study has shown insignificant changes are detected under surface tension influence. Thus one can conclude that, in the coating process the effect of surface tension is minor.

References

[1] A. Al-Muslimawi, Numerical analysis of partial differential equations for viscoelastic and free surface flows (PhD thesis), University of Swansea, 2013.

[2] E. Mitsoulis, Finite Element Analysis of Wire Coating, Poly. Eng. Sci. 26 (1986)171-186.

[3] E. Mitsoulis, R. Wagner and F. L. Heng, Numerical Simulation of Wire-Coating Low-Density Polyethylene: Theory and Experiments, Poly. Eng. Sci. 28 (1988) 291-310.

[4] F. Nadiri and R. T. Fenner, Performance of Extrusion Crossheads in Multi-Layer Cable Covering, Poly. Eng. Sci. 20 (1980) 357-363.

[5] C.D. Han, D. Rao, Studies on Wire Coating Extrusion. I. The Rheology of Wire Coating Extrusion, Poly. Eng. Sci. 18(13) (1978) 1019-1029.

[6] N. Phan-Thien, Influence of wall slip on extrudate swell: a boundary element investigation, J. Non-Newtonian Fluid Mech. 26 (1988) 327–340.

[7] B. Caswell, R.T. Tanner, Wirecoating die design using finite element methods, Poly. Eng. Sci. 18 (1978) 416- 421

[8] I. Sun, X-L Luo, R.I. Tanner, Theoretical and applied rheology, Proceedings XIth Int. Congr. on Rheol., Brussels (1992).

[9] P.B. Kuyl, 45th International Wire and Cable Symposium Proc, 736-742, (1996)

[10] P.B. Kuyl, Proceeding, ANTEC 97 (1997) 298-302.

[11] A.Al-Muslimawi, H.R. Tamaddon-Jahromi, M.F. Webster, Numerical computation of extrusion and draw-extrusion cable-coating flows with polymer melts, Appl. Rheol. 24 (2014) 34188.

[12] V. Ngamaramvaranggul, M.F. Webster, Simulation of coating flows with slip effects. Int.J.Num. Meth. Fluids 33 (2000) 961-992.

[13] A.Al-Muslimawi, H.R. Tamaddon-Jahromi, M.F. Webster, Numerical simulation of tube tooling cable coating with polymer melts, Korea-Aust. Rheol. J. 4 (2013) 197–216.

[14] I.C. Slattery, A.J. Giacomin, F. Ding, Wire coating by drawdown of an extruded annular melt, Int. Polym. Processing 2 (1999) 152-158.

[15] B. K. Jassim, A. Al-Muslimawi, Numerical analysis of Newtonian flows based on artificial compressibility AC method, J. of Al-Qadisiyah for computer science and mathematics, 9 (2017) 115-128

[16] A.J. Hade, A.J. Giacomin, Wire coating under vacuum, J. Eng. Mater. Technol. 123 (2001) 100-105.

[17] D.M. Hawken, H.R. Tamaddon-Jahromi, P. Townsend, M.F. Webster, A Taylor Galerkin based algorithm for viscous incompressible flow, Int. J. Num. Meth. Fluids 10 (1990) 327-351.

[18] R.I. Tanner, A theory of die-swell revisited, J. Non-Newt. Fluid Mech. 36 (2005) 85-87.

[19] A. Al-Muslimawi, Theoretical and numerical studies of die swell flow, Korea-Australia Rheology Journal 28(3) (2016) 229-236.